

Caldera events in a rift depocentre: an example from the Jurassic Neuquén basin, Argentina

LEANDRO D'ELIA¹* & JOAN MARTÍ²

¹*Centro de Investigaciones Geológicas (CIG), Universidad Nacional de La Plata–Consejo Nacional de Investigaciones Científicas y Técnicas (CONICET), La Plata B1900TAC, Argentina*

²*Instituto de Ciencias de la Tierra 'Jaume Almera', Consejo Superior de Investigaciones Científicas, Barcelona 08028, Spain*

*Corresponding author (e-mail: ldelia@cig.museo.unlp.edu.ar)

Abstract: We analyse the volcanic stratigraphy of the Lower Jurassic synrift sequence of the Sañicó depocentre, which is a sub-basin of one of the most important hydrocarbon basins in South America, the Neuquén rift basin. The Sañicó depocentre comprises a complex multicyclic volcano-sedimentary succession. The oldest part of the succession preserves a volcano-sedimentary sequence interpreted as the record of a stratovolcano. The middle part of the succession is characterized by the emplacement of two thick ignimbrites that completely filled the depocentre. Finally, the uppermost part of the succession records subordinate volcanism characterized by andesitic lavas associated with epiclastic sediments. The Sañicó depocentre shows a complex subsidence history that involves an interplay between tectonics and volcanism. During the early and late synrift phases, subsidence was relatively slow and permitted the accumulation of thick sequences of volcanic and sedimentary deposits throughout a long period of time. During the middle synrift phase, subsidence was very rapid and allowed the accumulation of a thick ignimbrite sequence in a very short time interval. In this study, this middle episode is interpreted as corresponding to a caldera-like event in which rapid subsidence occurred along the same normal faults that controlled tectonic subsidence during the previous and subsequent episodes.

Sedimentary rift basins constitute an essential target in exploration for mineral deposits and energy resources (Ziegler & Cloetingh 2004). They are characterized by extensional tectonics that generally leads to the formation of highly individualized, small depocentres that show a wide diversity of sedimentary environments (Schlische 1991, 1992; Howell & Flint 1996; Schlische & Anders 1996; Morley 1999; Gawthorpe & Leeder 2000; Jackson *et al.* 2005). The evolution of a rift basin may also be accompanied by profuse volcanic activity (e.g. Wilson *et al.* 1995; Rowland & Sibson 2001; Ziegler & Cloetingh 2004; Puskas *et al.* 2007), the effect of which over the stratigraphy of the rift successions may be considerable. Volcanism associated with extensional basins may show a wide range of compositions, eruptive styles and structures, from large calderas to monogenetic volcanic fields (e.g. Janecke *et al.* 1997; Best & Christiansen 2001; Spinks *et al.* 2005; Mora-Klepeis & McDowell 2004; Abebe *et al.* 2007; Aguirre-Díaz *et al.* 2008; Negrete-Aranda & Cañón-Tapia 2008; Rowland *et al.* 2010). The lithospheric structure and the extensional stress regime of the rift-ing areas are two of the most important factors that control the style and temporal–spatial distribution of magmatism and volcanism in these settings (e.g. Spinks *et al.* 2005).

Among the volcanic edifices that may occur in rift basins, collapse calderas are the ones that have a major impact on the structure and stratigraphy of the rift depocentres (Moore & Kokelaar 1998; Cummings *et al.* 2000; Colgan *et al.* 2008; Cole *et al.* 2010; Muravchik *et al.* 2011), as they may lead to the reactivation of extensional faults, create new structural elements (Acocella *et al.* 2004; Spinks *et al.* 2005), and supply a large amount of volcanic deposits to the depocentres in a very short time, causing an over-filled state (e.g. Muravchik *et al.* 2011). In the last two decades, many researchers have characterized various calderas developed in extensional and transtensional settings, showing their stratigraphic and structural complexities, such as contrasting eruption styles, incremental collapse, changes of the caldera depocentres between

succeeding collapses, departure from the typical caldera shape and absence of ring faults (Martí 1991, 1996; Moore & Kokelaar 1997, 1998; Acocella 2004, 2007; Spinks *et al.* 2005; Aguirre-Díaz *et al.* 2008; Cole *et al.* 2010; Petrinovic *et al.* 2010).

The initial Upper Triassic–Lower Jurassic volcano-sedimentary succession of the Neuquén rift basin has been interpreted as resulting from a complex multicyclic volcano-tectonic subsidence structure (Muravchik *et al.* 2011; D'Elia *et al.* 2012b). In this study, we analyse the stratigraphy of the synrift sequence in one of the depocentres of the Neuquén basin, the Sañicó depocentre (Fig. 1), showing how this sedimentary succession, which constitutes an important subsurface reservoir (see Pángaro *et al.* 2002; Legarreta *et al.* 2008; Pángaro *et al.* 2009), resulted from the superimposition of a major caldera collapse event on the normal tectonosedimentary evolution of the main basin. The evolution of the volcanic system is interpreted along with the tectonic evolution of the basin from the stratigraphy, facies analysis and structural constraints of the corresponding caldera-forming processes and related deposits.

Geological setting

The Neuquén basin is located on the eastern side of the Andean margin in central Argentina, between 32 and 40°S latitude (Fig. 1). The basin has a complex tectonic history that includes an initial Late Triassic–Early Jurassic extensional phase, the development of the Andean magmatic arc during its post-rift stage, and several basin inversion periods related to Andean tectonics, which occurred during Late Cretaceous and Cenozoic times (Vergani *et al.* 1995; Howell *et al.* 2005). The Late Triassic–Early Jurassic extension was related to widespread intracontinental rifting associated with the western margin of Gondwana (Franzese & Spalletti 2001; Franzese *et al.* 2003; Ramos 2009). Surface and subsurface studies, based on seismic records and well logs, demonstrated that the rift segments are elongated troughs 150 km long and 50 km wide, commonly composed of depocentres bounded by listric

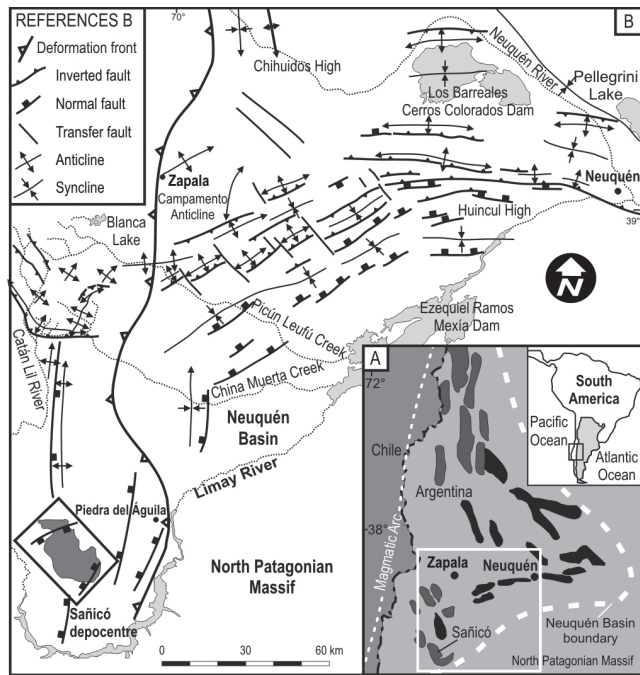


Fig. 1. Location maps. (a) Distribution of rift depocentres in the Neuquén Basin, Argentina (grey, exposed rift depocentre; black, rift depocentres in the subsurface). The white rectangle shows the areal extent of (b). Modified from Franzese & Spalletti (2001). (b) Map of the major structures recognized at surface and subsurface of the southern part of the Neuquén rift basin. Location of the Sañicó depocentre is highlighted with a black rectangle. Modified from Muravchik *et al.* (2011).

and planar faults, with half-graben geometries, showing alternating polarity (Vergani *et al.* 1995). The initial half-graben depocentres were associated with profuse volcanic activity (Franzese & Spalletti 2001), characterized by a variety of continental volcanic and volcanoclastic deposits (Franzese *et al.* 2006, 2007; Muravchik *et al.* 2011; D'Elia *et al.* 2012a), containing a large volume of cogenetic, calc-alkaline lava flows and pyroclastic deposits (D'Elia *et al.* 2012a). During the Early–Middle Jurassic post-rift thermal subsidence led to integration of the rifts into a single basin with widespread marine sedimentation. This period was combined with the onset of the subduction regime along the western margin of Gondwana, which in turn caused back-arc subsidence (Franzese & Spalletti 2001). Towards Late Cretaceous and Cenozoic times changes in the kinematics of the Andean subduction resulted in the development of the compressional tectonic regime that caused the inversion of several earlier extensional structures and the development of a foreland basin related to continental sedimentation (Howell *et al.* 2005).

The Neuquén basin has a broadly triangular shape and comprises two main regions: the Neuquén Andes (to the west), in which basin inversion caused the partial uplift and exposure of the basin infill as a result of the formation of a series of fold and thrust belts (Fig. 1a), and the Neuquén Embayment (to the east), where most of the sedimentary record is in the subsurface (Vergani *et al.* 1995; Howell *et al.* 2005). To the south of the Neuquén Andes, the initial volcanic rift successions show the best exposures. In this region, one of the exposed sub-basins corresponds to a highly compartmentalized half-graben 21 km wide, called the Sañicó depocentre (Muravchik *et al.* 2008; D'Elia *et al.* 2012a, b), which is the main focus of this study (Fig. 1). It is identifiable because its faulted margins were partially inverted and uplifted during the basin

inversion (Fig. 2a) that occurred in this part of the Andes mainly during Miocene time (Folguera & Ramos 2011), but that preserved its half-graben geometry (Fig. 2c). The dimensions and structural features of the Sañicó depocentre are comparable with those of other synrift depocentres documented in the subsurface. They show clear half-graben geometry with length of tens of kilometres, width from 10 to 20 km, and up to 2000 m of infill (Fig. 2d; Vergani *et al.* 1995; Pángaro *et al.* 2002, 2009).

Based on the varying ages of the successions with distinctive geometries related to the identified faults, the lithostratigraphic units involved in the evolution of the Sañicó depocentre could be divided into pre-rift, synrift and transitional post-rift units (Fig. 2a and b; D'Elia *et al.* 2012b). The pre-rift units are formed by igneous and metamorphic rocks including the Cushamen Formation (Volkheimer 1964) and the Mamil Choique Formation (Sesana 1968) of late Palaeozoic age (Varela *et al.* 2005). The synrift fill lies unconformably over the pre-rift units (Gulisano & Pando 1981; Franzese & Spalletti 2001) and comprises a thin succession of fluvial siliciclastic Upper Triassic deposits that are represented by the Paso Flores Formation (Frenguelli 1948; Morel & Ganuza 2002) and a Lower Jurassic thick succession of volcanic and volcanoclastic deposits (Sañicó Formation, Stipanovic 1967; Stipanovic *et al.* 1968). However, it is important to point out that most of the Paso Flores Formation lies outside the Sañicó depocentre. Also, the existence of a significant hiatus between this unit and the Sañicó Formation and the strong difference in lateral and vertical distribution between the two units suggest that the Paso Flores Formation should not be included in the synrift evolution of the Sañicó depocentre (see D'Elia *et al.* 2012b). Therefore, this paper concentrates only on the analysis of the Sañicó Formation.

The Sañicó Formation mainly consists of lava flows and pyroclastic and epiclastic deposits (Galli 1969). Although the stratigraphy of these deposits suggests a Hettangian–Sinemurian age (Stipanovic 1967; Stipanovic *et al.* 1968), a geochronological study, as well as high-resolution ammonite biozonation (precision of c. 500 ka; for a review see Howell *et al.* 2005), established an accurate chronostratigraphic framework for the volcanic synrift sequence of this depocentre. Spalletti *et al.* (2010) dated the lower part of the synrift sequence to a U–Pb sensitive high-resolution ion microprobe (SHRIMP) age of 191.7 ± 2.8 Ma, whereas Damborenea & Manceñido (1993), on the basis of ammonite biozonation, constrained the lower marine deposits of the transitional post-rift units to Early Pliensbachian age ($c. 189.6 \pm 1.5$ Ma). This scheme establishes a maximum period of deposition for the Sañicó Formation of c. 4 Myr. It is important to mention that only a few radiometric data are available for the synrift succession (see Schiuma & Llambías 2008; Spalletti *et al.* 2010) and that the U–Pb SHRIMP method shows an error margin of 2.8–1.5 Ma (see Schiuma & Llambías 2008; Spalletti *et al.* 2010). Thus it is unlikely to establish an accurate chronostratigraphic framework when discussing events of limited duration such as caldera cycles, in which magma residence times calculated for various caldera systems worldwide are around 4–19 kyr to 300–500 kyr (for a review see Costa 2008).

The transitional post-rift units correspond to the Lower–Upper Pliensbachian marine succession (Damborenea & Manceñido 1993) of the Piedra Pintada Formation (Stipanovic *et al.* 1968; Stipanovic 1969). It consists of a marine siliciclastic-dominated succession (Galli 1969; Gulisano & Pando 1981) that is mainly composed of a thick succession of massive to millimetre-scale laminated mudstone with ammonite and bivalve fossils and plant remains. It overlies the Sinemurian volcanic and volcanoclastic succession of the Sañicó Formation showing either concordance or angular-erosive discordance, which represents a short time-lapse (D'Elia *et al.* 2012b).

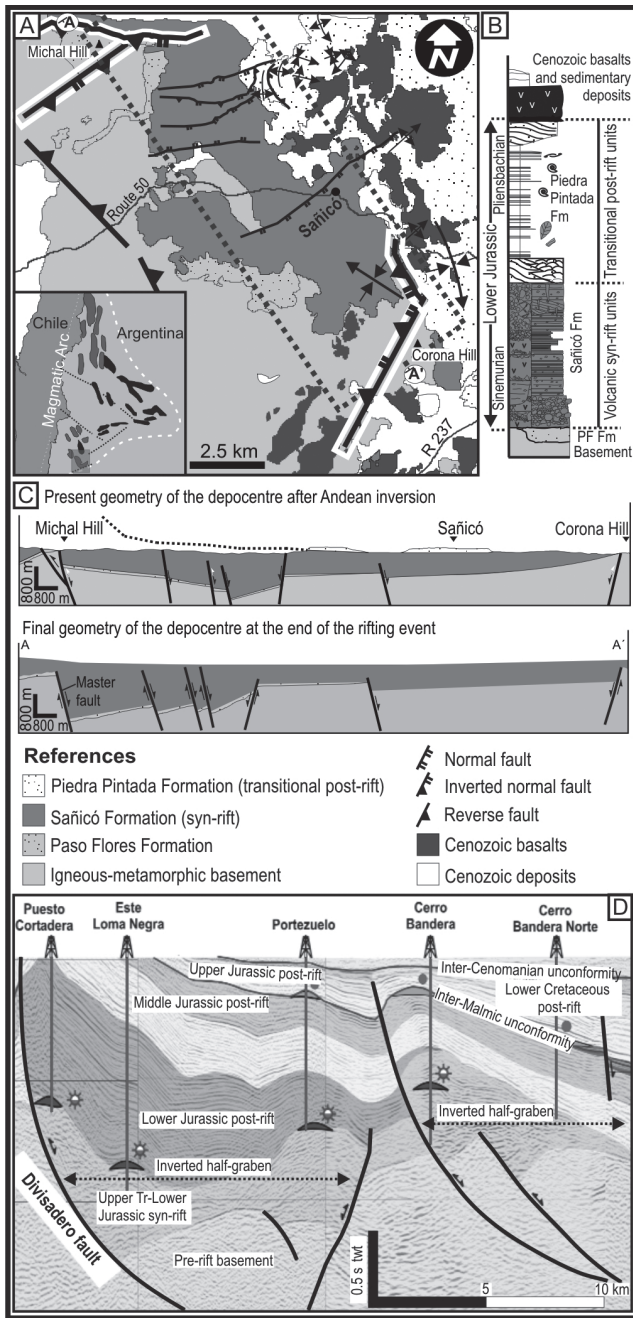


Fig. 2. (a) Simplified geological maps of the study area. Dotted rectangle indicates the detailed geological map shown in Figure 3. (b) Schematic stratigraphic column representing the units in the Sañicó area. (c) Present and restored cross-sections of the Sañicó depocentre at the end of the rifting event. (d) Interpretation of the seismic lines, showing the half-graben depocentres on the subsurface of the Huincul High area. Modified from Pángaro *et al.* (2002; see Fig. 1 for location).

Methods

The study of the volcanic synrift succession was carried out through detailed structural and geological mapping, which included the construction of nine stratigraphic sections that provided accurate information on the entire depositional area (Fig. 3). It is important to highlight that all of the tectonic structures described in this study are related to the synrift extension and that many of them were partially

reactivated during the positive inversion (for reviews see Cooper & Williams 1989; McClay 1995) that occurred during Miocene time (Folguera & Ramos 2011), so extensional faults were reactivated in the opposite sense to their original movement, partially uplifting and deforming the synrift strata but preserving the original strike and dip. New faults that originated during the Andean orogeny were mapped, but they were not analysed in the study (Figs 2 and 3). A geographic information system (ArcGIS 9.3®) was used to manage geodata, such as digital elevation models, remote sensing images and derived spatial information (maps, cross-sections, etc.). The relative abundance of lava, pyroclastic deposits and sedimentary rocks and their minimum volumes were estimated by weighting the thickness variations deduced from the stratigraphic logs and the areal distribution. Stratigraphic and sedimentological analysis of the pyroclastic units allowed us to distinguish several lithofacies using classical facies models applied to pyroclastic deposits (see Branney & Kokelaar 2002; Németh & Ulrike 2007; Sulpizio & Dellino 2008). Lateral and vertical facies associations were established by the correlation of the stratigraphic sections, using the transitional post-rift succession as a regional marker horizon. The compositional and textural characteristics of the pyroclastic rocks were studied through thin-section image analysis. Provenance analysis was performed directly in the field and later combined with the microscopic inspection of samples.

Stratigraphy of the Sañicó Formation

The stratigraphy of the Sañicó Formation has been established in detail in previous studies (Galli 1969; Gulisano & Pando 1981; D'Elia *et al.* 2012*b*). The synrift sequence of the Sañicó depocentre is mainly made up of subaerial calc-alkaline lavas, pyroclastic rocks, volcanogenic sedimentary rocks and shallow intrusions (D'Elia *et al.* 2012*a, b*). The fault system of the Sañicó sub-basin controlled the accumulation of a thick synrift succession, mainly to the north of the study area. Figures 2, 3 and 4c show how the master fault of the depocentre, which at present is partially inverted, separates a thin succession composed of lava flows to the NW from a thick synrift succession with more than a thousand metres of volcanic, pyroclastic and sedimentary rocks to the SE (Figs 3 and 4a). To the SE of this master fault, the synrift succession can be traced for 21 km to the other margin, which also is a partially inverted margin, where the synrift succession is absent or reaches its minimum thickness (Figs 2 and 3). Lava and pyroclastic rocks represent up to 72% of the total of the Sañicó Formation and share a comagmatic trend, ranging in composition from basaltic andesite to rhyolite, dominated by intermediate to silicic rocks (D'Elia *et al.* 2012*a*). The sedimentary facies form up to 28% of the volcanic synrift succession and mainly correspond to epiclastic volcanogenic deposits mostly derived from sediment gravity flows and, to a lesser extent, lacustrine carbonate deposits (D'Elia *et al.* 2012*b*).

According to the stratigraphic relations between the units and the relative proportion of volcanic and sedimentary rocks (Fig. 4b), and also of components in the pyroclastic deposits (Fig. 4a), three main stratigraphic members were distinguished from base to top in the Sañicó Formation, which are separated by unconformity surfaces (i.e. Lower, Middle and Upper members; Figs 3 and 4a). Volcanic rocks are volumetrically the most important units in the Lower and Middle members, whereas they are less abundant in the Upper Member (Fig. 4b). The most conspicuous feature of the Sañicó depocentre is the Middle Member, which is mostly composed of laterally continuous, thick rhyolitic or rhyodacite pyroclastic flow deposits (which form more than 95% of the volume of this member; Figs 3 and 4). Therefore, to establish the volcanic stratigraphy of the Sañicó Formation, we analysed the three members, paying special attention to the Middle Member, in which a detailed facies and architectural analysis was carried out.

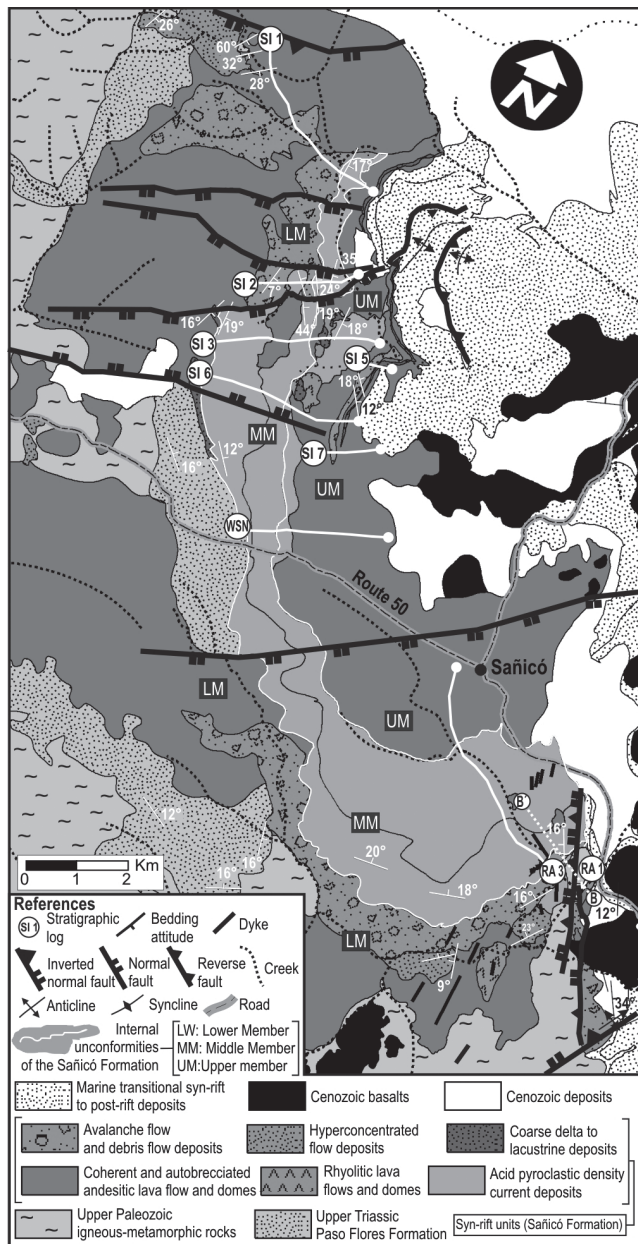


Fig. 3. Detailed geological map of the Sañicó depocentre and location of stratigraphic logs shown in Figure 4. Track of the logged sections is indicated with white lines.

Lower Member

The first episodes in the deposition of the Sañicó Formation are characterized by lava units (which form up to 61% of the total volume of this member), volcanogenic sediments and minor silicic pyroclastic deposits, all intruded by andesitic dykes and dacitic-rhyodacitic necks and cryptodomes (Fig. 4a and b). This member is wedge-shaped along the cross-section perpendicular to the boundary faults, where it reaches the greatest thickness (Fig. 4a and c), and has onlapping and irregular contacts with the pre-rift rocks towards the SW margin of the depocentre, where the faults show a lateral decrease in displacement (Fig. 3; D'Elia *et al.* 2012b). Through the depocentre this member has important thickness variations controlled by the inner faults (Fig. 4a and c) and discernible

facies arrangements. The footwall basement blocks of the depocentre are overlain by a thin succession of coherent and auto-brecciated intermediate lava flows, whereas in the hanging walls there is a more complex arrangement formed mainly of lava flows, and pyroclastic and sedimentary deposits (Figs 3 and 4a). Towards the base, this member is mainly formed by a thick succession of coherent and auto-brecciated intermediate lava flows and lava domes (Figs 3, 4a and 5a–c), and to a lesser extent by low-volume dacitic pyroclastic flow deposits (Fig. 3). Two groups of gravity flow deposits, mostly composed of andesitic clasts, are present towards the top and inside the depocentre. One of them consists of large volcanic debris avalanche deposits (Fig. 5e) and lens-shaped debris flow deposits (Fig. 5f), whereas the other is formed by channelized volcanoclastic alluvial units (Fig. 3), mainly composed of gravelly and sandy hyperconcentrated flow deposits (Fig. 5g; *sensu* Smith 1986, 1987; Smith & Lowe 1991). Close to the boundary of the depocentre all of these units were intruded by intermediate dykes, felsic necks and domes (Figs 3 and 5d).

Middle Member

The middle part of the Sañicó Formation corresponds to a thick succession of more than 400 m, composed of silicic ignimbrites that unconformably overlie the previous units at a sharp regional stratigraphic discontinuity (Fig. 6). This ignimbrite sequence consists of two ignimbrite units (Unit A and Unit B) and was identified only inside the depocentre (Fig. 3). It has a minimum estimated volume of 20 km³ and shows thickness variations associated with the relative displacement of the internal faults, being ponded against the boundary faults of the depocentre (Figs 3, 4, 7 and 8a). The ignimbrites are continuous throughout the interior of the depocentre (Figs 3 and 4a) and are separated by thin hyperconcentrated flow deposits that are interpreted as syneruptive volcanoclastic deposits (Figs 4a and 8b). Unit A has an outcrop length of 21 km within the depocentre with a maximum thickness of 140 m (Fig. 7a). Unit B is also exposed with lateral continuity throughout the depocentre, but shows lesser thickness variations than Unit A. It has a maximum thickness of 270 m at the centre of the depression (Fig. 7b).

The ignimbrite units show very similar lithological and sedimentological characteristics. They contain 0.5–3 cm pumice clasts surrounded by an abundant ash matrix, and show post-depositional devitrification and alteration. Towards the base they generally show sericite–chlorite alteration (Fig. 8c), whereas towards the top they usually show pervasive silicification, including both vapour-phase crystallization and deuteric alteration (Fig. 8d), as well as gas pipe structures (Fig. 8e). Sericite–chlorite alteration consists of replacement structures, coated glass surfaces and infill textures, which may or may not obliterate the primary fabrics (Fig. 8c), whereas both the vapour-phase crystallization and deuteric alteration generally preserved shard morphologies (Fig. 8d). The matrix changes from slightly packed with some adhesion between shards and no coalescence of glassy materials to moderately packed in which shards are only slightly deformed where clasts are moderately adhered to one another (Fig. 8d). The pumice lapilli vary from randomly oriented with no deformation to moderately deformed and fully collapsed fiamme forming a clear eutaxitic texture. The cognate crystal fragments are quartz, K-feldspar, plagioclase and biotite (Fig. 8c and d). Lithic fragments of Palaeozoic igneous and metamorphic rocks and diverse volcanic rocks, mainly of intermediate composition, are present.

The ignimbrite units may show several lithofacies, depending on the relative proportion and size of juvenile and lithic fragments, matrix textures and the presence of sedimentary structures. The main ignimbrite bodies are characterized by moderately to poorly sorted lapilli-tuff facies (Fig. 8f and g) composed of pumice lapilli

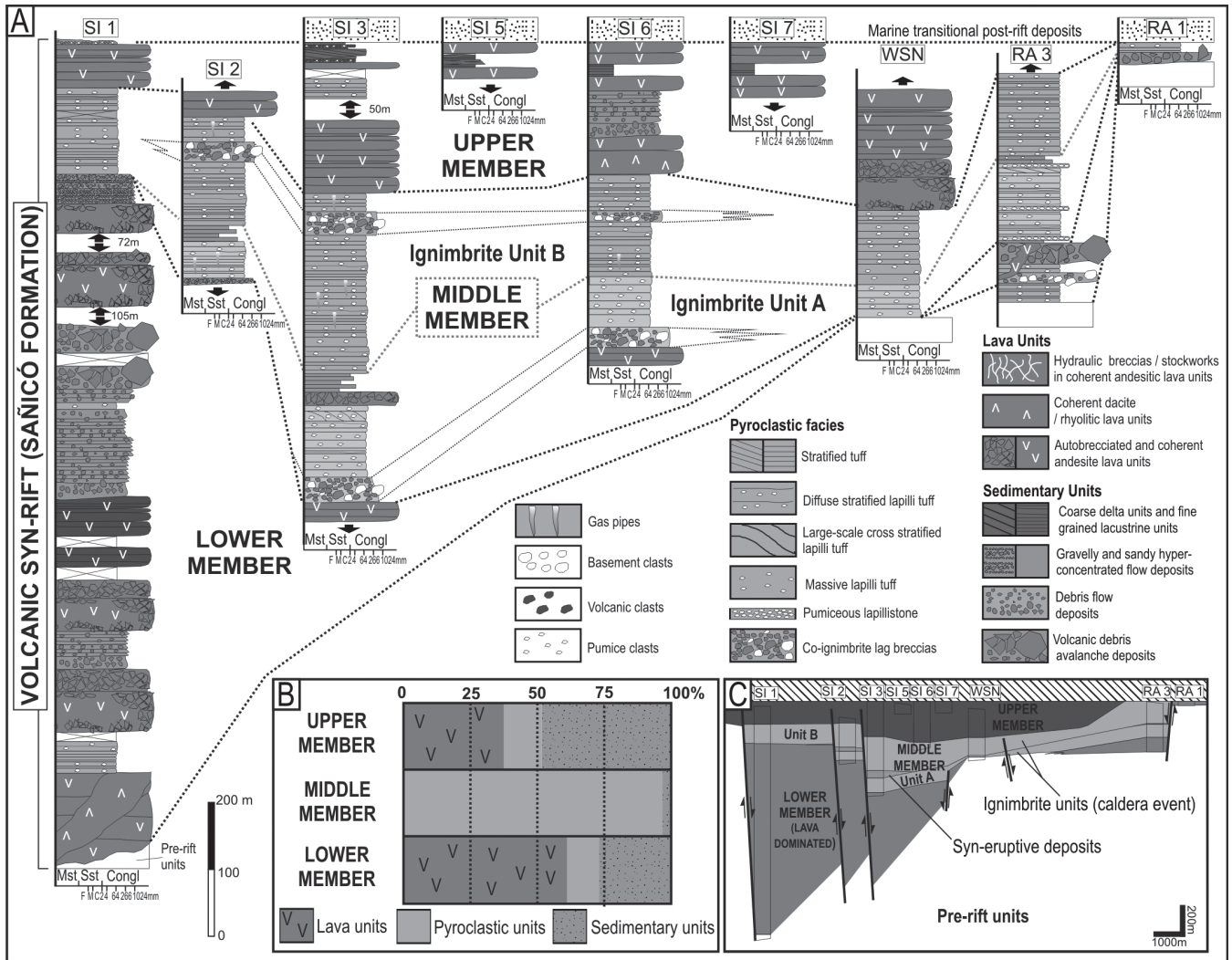


Fig. 4. (a) Stratigraphic logs of the synrift succession of the Sañicó depocentre. Mst, mudstones; Sst, sandstones; Congl, conglomerates; F, fine; M, medium; C, coarse. (For location of the stratigraphic logs see Fig. 3.) (b) Percentages of lava, pyroclastic and sedimentary products estimated for each member. (c) Schematic correlation between stratigraphic logs of the Middle Member and the structural control on the synrift sequence.

(up to 7 vol%), cognate crystal fragments (3%–25 vol%) and lithic fragments (3–15 vol%), in an abundant tuff-matrix (90–70 vol%), which is mainly formed of juvenile fragments (Fig. 8c and d). The lapilli-tuff shows massive or oriented fabrics, which represent rapid aggradation from a high-concentration fluid escape-dominated (with or without a component of granular flow) depositional flow boundary of a pyroclastic density current (see Branney & Kokelaar 2002; Sulpizio *et al.* 2007). Both units typically contain toward their bases (Fig. 9a) or middle parts (Fig. 9b) horizons of up to 30 m thick of clast-supported to matrix-supported lithic breccias, with polymodal sorting (Fig. 9c) and scarce matrix (up to 25 vol%) formed by juvenile and lithic fragments (Fig. 9d). These lithic breccias contain angular to subrounded lithic clasts of several centimetres to decimetres in size of both accessory (i.e. andesites) and accidental material (i.e. substrate-derived rocks). These breccia facies may correspond to co-ignimbrite lag breccia deposits formed during the vent opening or vent enlargement phases (Wright & Walker 1977; Druitt & Sparks 1982; Pittari *et al.* 2008). In some places, especially toward the base, the ignimbrite units show stratified tuff facies. Small-scale stratified facies (Fig. 8g) indicate deposition from the traction-dominated flow boundaries of a pyroclastic density current (Cas &

Wright 1987; Branney & Kokelaar 2002; Sulpizio *et al.* 2007), whereas large-scale cross-bedding (Fig. 8f) is occasionally present over erosive surfaces, thus suggesting progradation and retrogradation of the pyroclastic flow over hydraulic jump structures that originated from unsteadiness in the current (Branney & Kokelaar 2002).

Lateral and vertical facies variations are usually gradual (Fig. 4), thus suggesting that the different facies correspond to small variations in the vent conditions and/or emplacement of pyroclastic flows rather than to drastic modifications in the eruption conditions (see Allen & Cas 1998; Allen *et al.* 1999; Allen 2001; Pittari *et al.* 2008). Also, the absence of internal sharp discontinuities in these ignimbrites suggests that the eruptive episodes that gave rise to their emplacement were continuous. However, internal layering, defined by externally crude stratification, may be interpreted as corresponding to a progressive aggradation emplacement of the ignimbrites, in the sense defined by Branney & Kokelaar (2002).

Upper Member

The upper part of the Sañicó Formation succession unconformably overlies the Middle Member (Fig. 4a) and is marked by a decrease

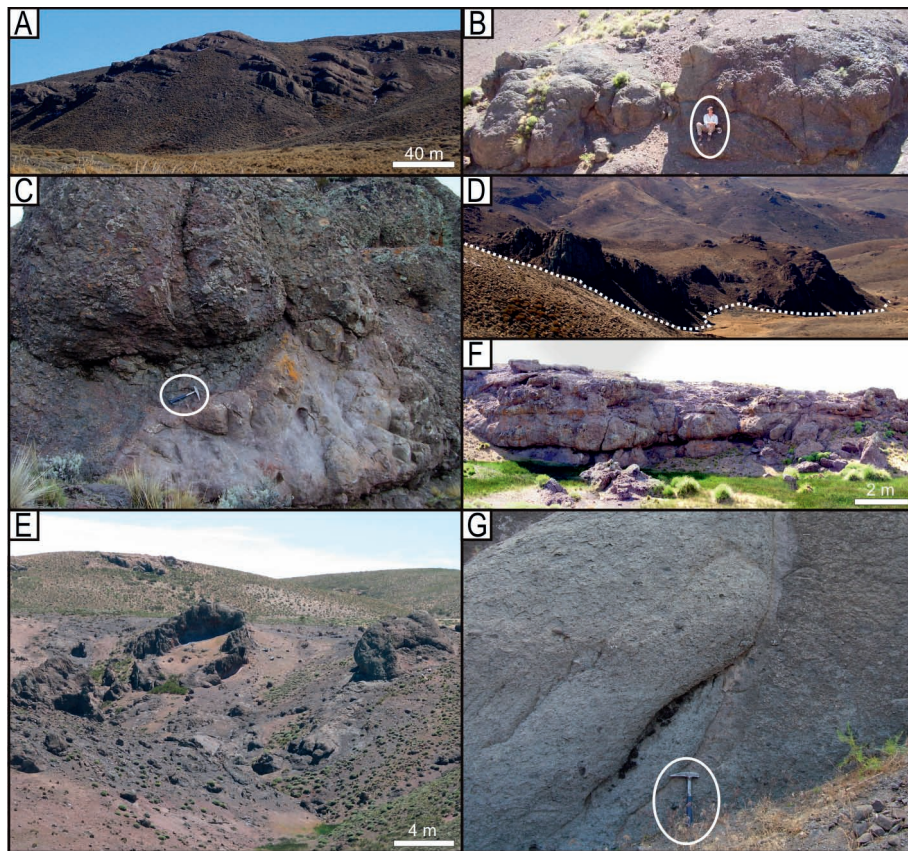


Fig. 5. Volcanic and sedimentary units of the Lower Member. (a) Outcrop-scale photograph of the andesitic lava flow succession. (b) Brecciated andesitic lava forming a small lava dome (oval indicates person for scale). (c) Coherent and brecciated andesitic volcanic facies in a lava flow (oval indicates hammer for scale). (d) Neck of dacitic lava. (e) Outcrop-scale photograph of massive matrix-supported to clast-supported breccias formed by volcanic debris avalanches. (f) Lobate body successions composed of massive matrix-supported conglomerates deposited by debris flows. (g) Sandy and gravelly hyperconcentrated flow deposits (oval indicates hammer for scale).

in the volume of volcanic rocks (<52%; Fig. 4b), as well as a reduction in its total thickness and lateral extent compared with the preceding ignimbrite units (Fig. 4a and c). Although to a lesser extent, extensional tectonics also affected this member (D'Elia *et al.* 2012b), as is indicated by thickness changes in the successions across the inner faults, as well as changes in the accommodation areas with respect to the previous members (Fig. 4). This member is composed of andesitic lava flows with profuse hydrothermal alteration (Fig. 10a) with associated epiclastic and carbonate sedimentary deposits, which are asymmetrically distributed within the depocentre. The epiclastic deposits correspond to delta systems formed by coarse-grained successions (Fig. 10b), which towards the interior of the depocentre turn into a thin succession of limestones and fine-grained siliciclastic lacustrine deposits (Fig. 10c and d; D'Elia *et al.* 2012b). To a lesser extent, silicic lava domes mainly related to the boundary tectonic structures and minor pyroclastic deposits are also present (Fig. 11).

Structural features of the Sañicó depocentre

As pointed out above, the Sañicó rift depocentre is clearly identified from the stratigraphic analysis of its infill, as well as by its faulted margins (D'Elia *et al.* 2012b). The Sañicó Formation has a thickness of up to 1700 m at the NW boundary (i.e. the master fault system), whereas at the SE boundary of the depocentre it is only up to 600 m thick. This evidence suggests a half-graben geometry for the Sañicó depocentre (see Schlische 1991, 1992; for a review see Schlische & Anders 1996). Several of the Lower Jurassic normal faults were inverted (i.e. thick-skinned thrust; Fig. 6a) during the Andean deformation, which occurred mainly in the Miocene (for a review see Howell *et al.* 2005).

The boundaries of the depression are shown as basement-core emergent anticlines (i.e. classical inversion geometry; for a review see McClay 1995), forming NE–SW-oriented folds with ENE–WSW- and NNW–SSE-trending overlapping structures (Figs 2 and 3). Within the depocentre, extensional or partially inverted normal faults, parallel and oblique to the margin structures, have also been identified (Fig. 11a and b).

Detailed mapping of the Sañicó Formation units was carried out to identify the distribution and magnitude of the Mesozoic extensional structures (Fig. 3). High-angle major faults and associated medium-scale faults, with NE–SW, ENE–WSW and, to a lesser extent, NNW–SSE trends, were measured in the interior and at the borders of the Sañicó depocentre; all of these faults controlled the general orientation of the basin and the thickness variations of the infilling deposits (Figs 3 and 11b). They are commonly spaced 0.1–3 km apart, showing lengths ranging from 3 to 8 km and the predominance of dip-slip movement with displacement of tens to hundreds of metres (Figs 3, 6a and 7). These faults played a significant role during the deposition of the entire Sañicó Formation, controlling the subsidence of the basin, in particular during the deposition of the Middle Member ignimbrite units (Figs 4a, c and 7a, b). This is indicated by the fact that they were preferentially deposited in the interior of the depocentre and ponded against the boundary faults. The thickness differences recorded, from tens to hundreds of metres across the faults (Fig. 7), are unlikely to reflect a passive infill of a depression, because of the sharp depocentre-scale erosive surface that separates the Lower Member from the Middle Member, which suggests the existence of a long depositional hiatus, indicating that such fault scarps would not have been so well preserved. It is important to point out that ductile deformation of the ignimbrite along the faults (e.g. deflection of eutaxitic

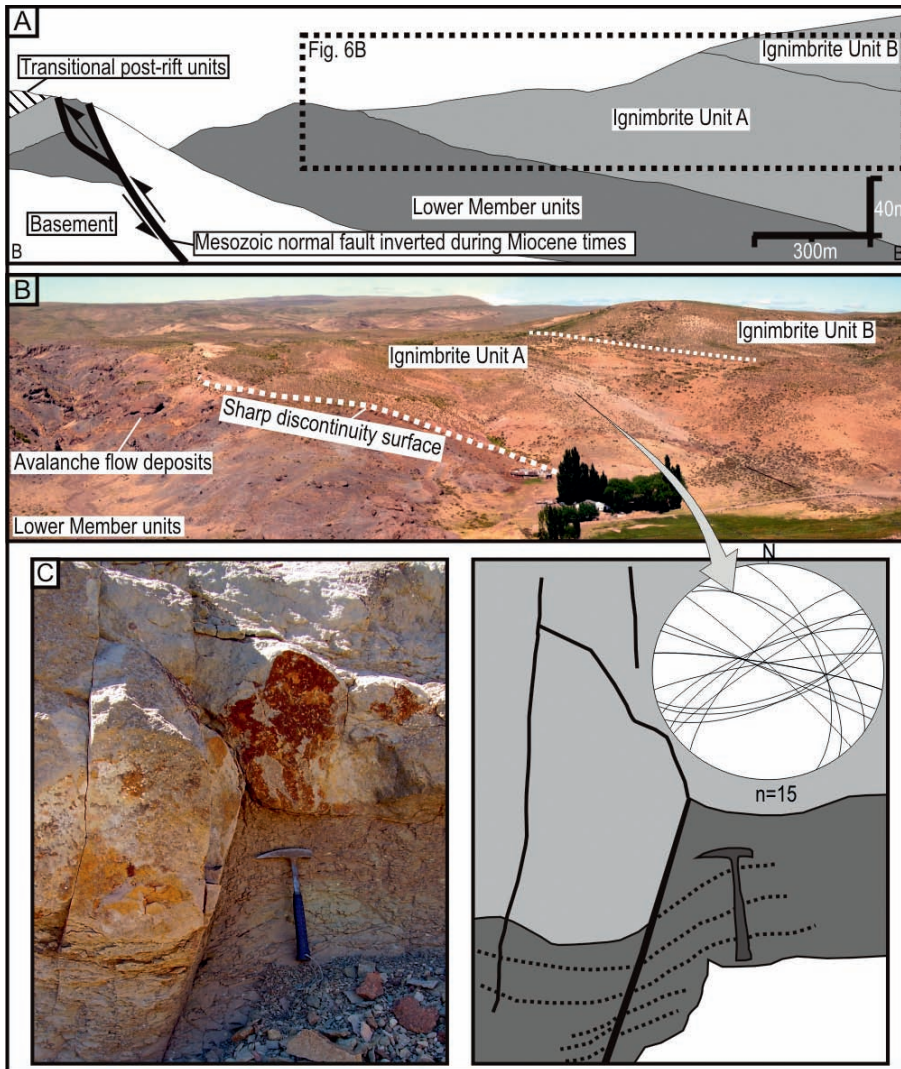


Fig. 6. (a) Cross-section showing a Mesozoic extensional fault, which acted as a volcano-tectonic fault during the caldera-forming event, inverted during the Andean orogeny in Neogene times (see Fig. 3 for location). (b) Outcrop-scale photograph of the hanging wall sequence (see dotted rectangle in (a) for location), in which the sharp contact between the avalanche flow deposits of the Lower Member and Unit A of the Middle Member of the Sañicó Formation can be appreciated. (c) Small-scale syndepositional extensional faults developed in Unit A close to the major fault plane.

foliation and large-scale flows), which in other areas was mentioned by some researchers as evidencing volcano-tectonic faulting (e.g. Branney & Kokelaar 1994), was not recognized here. Such structures were recorded in high-grade or rheomorphic ignimbrites, which do not represent the ignimbrites under study. Also, in the present case, major fault zones were significantly modified during the inversion tectonics (Fig. 6a). Nevertheless, close to the major faults, small-scale extensional faults were identified (Fig. 6c), which decrease in intensity with distance from them. They are commonly spaced 2–10 m apart, with multidirectional trends that affect only an ignimbrite stratum or pass into diffuse shear and lose their identity. In some cases the oriented fabrics of ignimbrite strata affected by small-scale faults show gentle drag folds (Fig. 6c). This indicates that these originated before pervasive cementation occurred by post-emplacement alteration, indicating that small-scale faults, associated with major faults, were active during the ignimbrite deposition (see Branney & Kokelaar 1994). These observations are consistent with the large thickness variations of the ignimbrite units across the inner faults where progressive changes of the attitude of strata were recorded, indicating rotation of the fault block during deposition (Figs 3, 4c and 7), which provides further evidence that subsidence occurred synchronously with the deposition of the ignimbrites.

Other structures that are relevant to understanding the volcano-tectonic evolution of the Sañicó depocentre correspond to intrusion of intermediate and silicic intrusive bodies that intersect the infill sequences at different levels, mainly emplaced along pre-existing extensional faults (Fig. 11). On the one hand, N147°- and N171°-trending andesitic dyke swarms with a maximum length of <6 km and a width of 0.5–2.5 m for each dyke (Fig. 11c) were recognized, mostly intruding the Lower Member of the Sañicó Formation, whereas NNW–SSE-trending intrusive felsic bodies, of tens of metres width (Fig. 11f and g), and lava domes related to ENE–WSW-trending intra-basin fractures were also observed (Fig. 11d and e) intruding the Sañicó Formation. Thus, the volcanic feeder system of andesitic volcanism that characterizes the Lower and Upper Member of the Sañicó Formation used the tectonic structures that controlled the subsidence of the basin (Fig. 11c). Although the silicic vents were also mainly controlled by boundary tectonic structures of the depocentre, they occurred as more restricted and wider conduits (Fig. 11d–g). In the Middle Member, ignimbrite dykes or subvertical discordant ignimbrite bodies, which have been mentioned in other extensional basins associated with volcano-tectonic processes as ignimbrite vents (e.g. Branney & Kokelaar 1994; Aguirre-Díaz *et al.* 2008), were not recognized here. We infer that silicic necks and lava domes, located mainly at

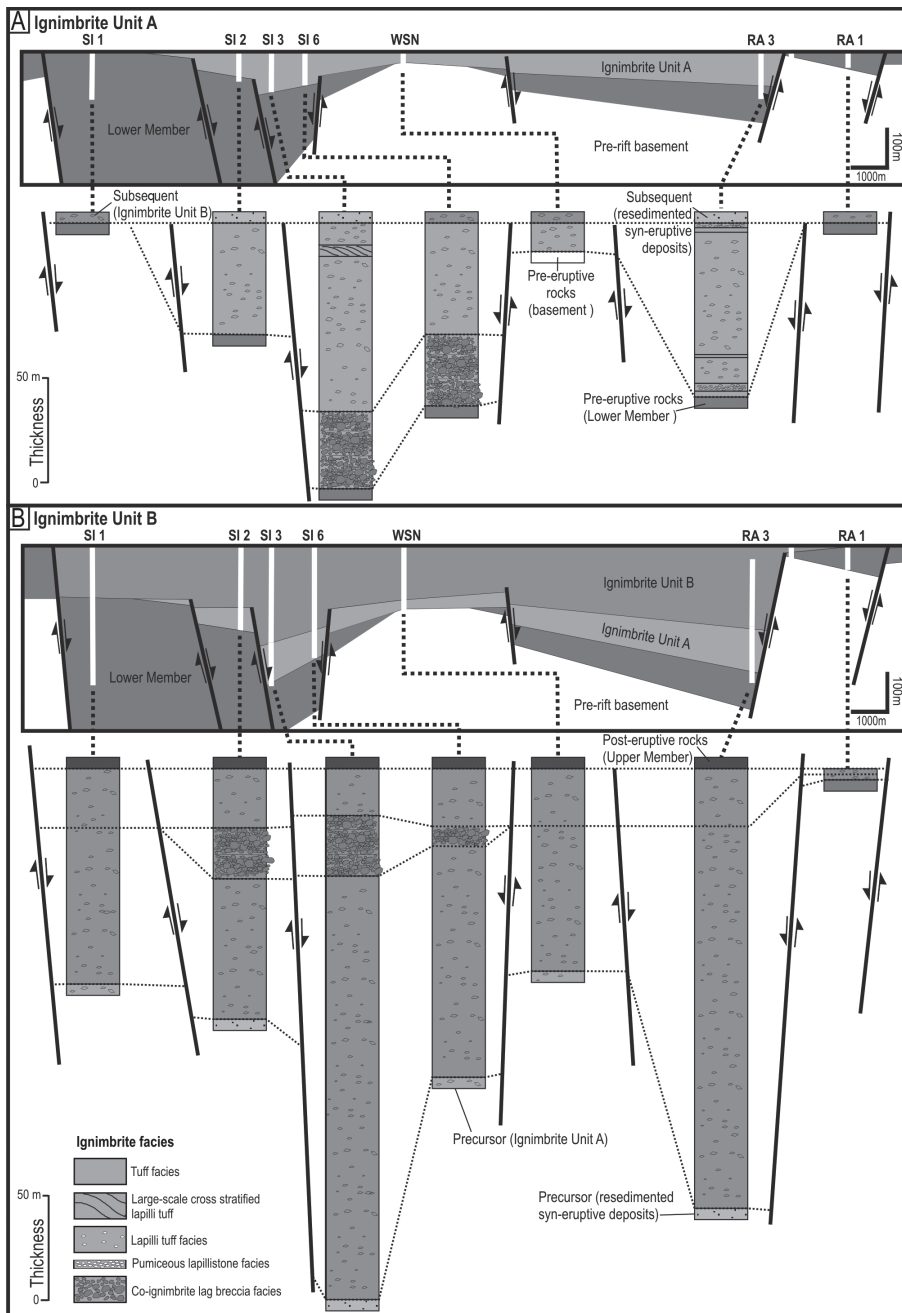


Fig. 7. (a, b) Longitudinal correlation panels of Units A and B, showing major thickness changes across the extensional fault, indicating that these were active as volcano-tectonic faults during the caldera-forming event. In the fence diagrams, the facies changes of the ignimbrite units can be appreciated, especially the lag breccia facies developed against the faults. Dotted lines indicate the correlation between the facies and the sections established. Location of the extensional faults is based on the geological map in Figure 3. **(a)** is level with the top of Unit A, whereas **(b)** is level with the top of Unit B.

the boundary of the depocentre, could represent the ignimbrite vents plugged during post-eruptive stages. This is well correlated with the ignimbrite facies distribution (Fig. 7).

The locations of the sub-volcanic bodies as well as the distribution of tectonic structures reflect the structural complexity of the Sañicó depocentre during the synrift evolution, where NE–SW- and ENE–WSW-trending pre-existing fabrics of the basement (see Varela *et al.* 1991) were active, along with extensional structures related to the regional orientation of the stresses (D'Elia *et al.* 2012b), and both were reactivated during the emplacement of the Middle Member as volcano-tectonic structures controlling both magma eruption and basin subsidence. Therefore, the Sañicó depocentre constitutes one of the typical extensional depocentres of the Neuquén basin, formed in the setting of an oblique rift system (for a review see Moustafa 2002; Morley *et al.* 2004), as was recently suggested by some researchers

(Cristallini *et al.* 2006; Giambiagi *et al.* 2008; Bechis *et al.* 2010), and was profusely affected by volcanism.

Discussion

One of the most important issues addressed in this study is the close relationship that existed between volcanism and extensional tectonics during the evolution of the Sañicó depocentre. In particular, the dramatic thickness variations across the extensional faults, the stacking of lithic breccias against the faults, and the small-scale syndepositional faults adjacent to major faults suggest that previous tectonic structures were reactivated as volcano-tectonic faults that controlled the rapid subsidence during the emplacement of the Middle Member.

The Sañicó Formation is a synrift succession composed of up to 72% of volcanic products in which three main stages or members

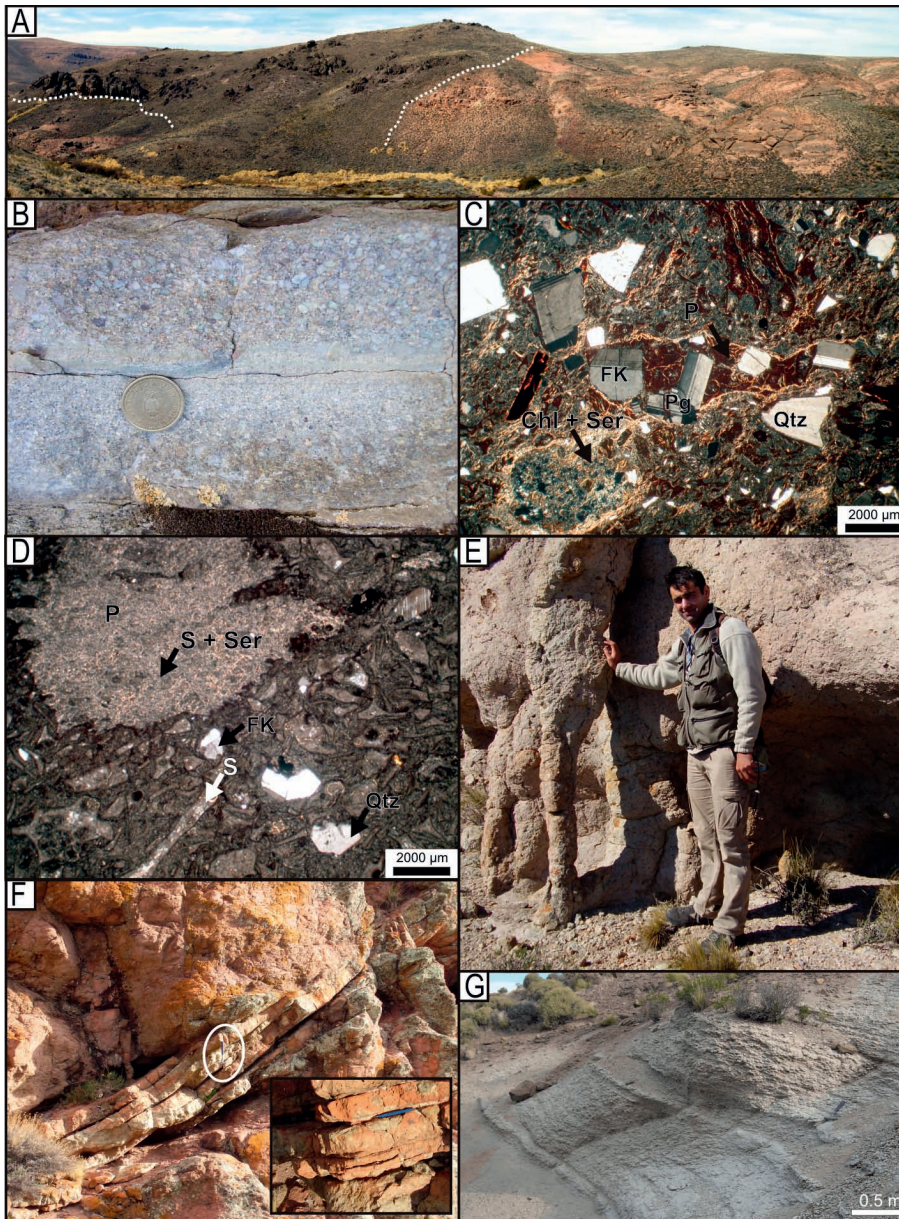


Fig. 8. Volcanic and sedimentary units of the Middle Member. (a) Outcrop-scale photograph of Unit A intruded by andesitic lava dome. (b) Sandy hyperconcentrated flow deposits occurring in inter-eruptive stages between Units A and B. (c) Microphotograph of the ignimbrite with pervasive chlorite-sericite alteration (P, recrystallized pumice clast; Chl, chlorite; Ser, sericite; Qtz, quartz; FK, K-feldspar; Pg, plagioclase). (d) Microphotograph of the ignimbrite with pervasive silicification resulting from both vapour-phase crystallization and deuteric alteration (S, recrystallized shards). (e) Outcrop-scale photograph of gas pipe occurring at the top of Unit B. (f) Outcrop-scale photograph of the large-scale cross-stratified lapilli-tuff facies, developed in Unit A. (g) Lapilli-tuff facies with horizontal stratification, occurring at the base of Unit A.

can be identified based on the existence of major stratigraphic discontinuities between members and significant differences in the proportion and nature of volcanic rocks among them. Each member is characterized by a different type of volcanism with different eruptive characteristics and location and geometries of volcanic vents. Whereas dyke-related andesitic volcanism alternating with sedimentary episodes that characterized the Lower and Upper members are mainly associated with effusive volcanism, the Middle Member corresponded to highly explosive events that erupted two voluminous ignimbrites through the major faults that were controlling basin subsidence, completely filling the depocentre.

Structural reconstruction and facies analysis have allowed us to infer that the master and inner faults controlling formation and tectonic subsidence of the depocentre during the deposition of the Lower and Upper members played a major role during these ignimbritic episodes. They acted as vent sites for the eruption of the ignimbrites and controlled the rapid subsidence of the depocentre and, therefore, the distribution and thickness variations of these pyroclastic deposits (Figs 4a, c and 7). Some facies variations shown by the ignimbrites are clearly

related to the syndepositional movement of the faults that controlled the subsidence of the basin (Fig. 7a and b). The intraformational breccias that appear at the base of the ignimbrite units may be interpreted as co-ignimbrite lag deposits, which mostly developed at the marginal zones of the sub-basin and gradually decreasing in thickness towards the interior of the depocentre (Figs 4a and 7a, b).

Similar observations to those above have been considered by various researchers as indicative of caldera-like episodes in several ancient and recent volcanic sequences occurring in transpressional or extensional basins (e.g. Martí 1991, 1996; Branney & Kokelaar 1994; Moore & Kokelaar 1997, 1998; Cole *et al.* 2005; Spinks *et al.* 2005; Aguirre-Díaz *et al.* 2008; Petrinovic *et al.* 2010). Therefore, the Sañicó sub-basin may be interpreted as another example of a caldera-like structure, related to calc-alkaline volcanism in an extensional setting, as there is a clear pre-existing tectonic control on caldera subsidence instead of a typical ring fault system formed by decompression of a magma chamber (for a review see Martí *et al.* 2009).

In summary, the evolution of the Sañicó sub-basin began with the deposition of the Lower Member of the Sañicó Formation, which was

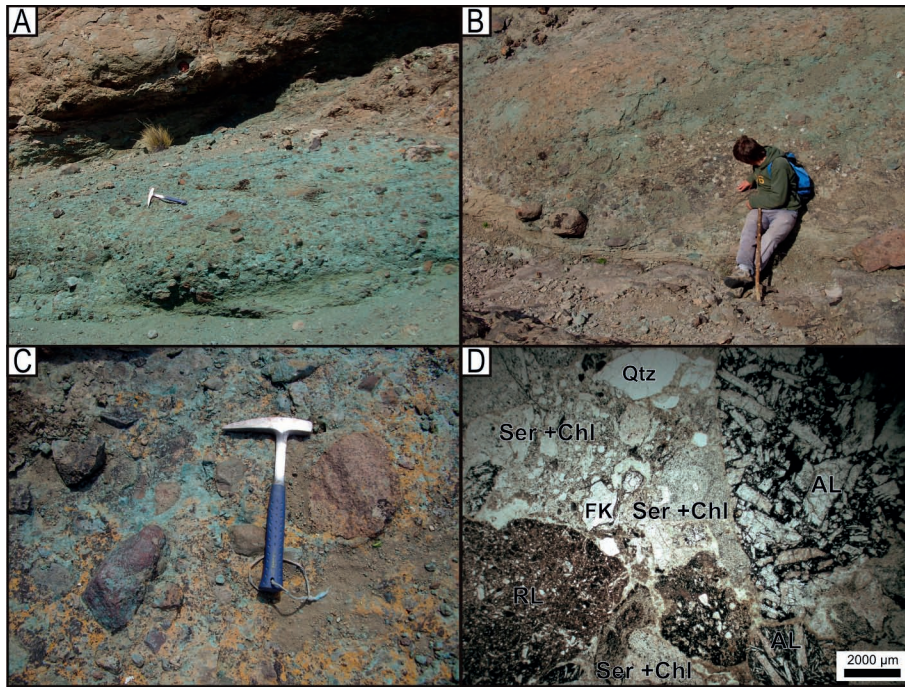


Fig. 9. (a, b) Co-ignimbrite lag breccias developed at the base of Unit A (a) and in the middle part of the Unit B (b). (c) Detail of clast-supported, polymodal sorting, co-ignimbrite lithic breccias. (d) Microphotograph of matrix of the co-ignimbrite lag breccias (Ser + Chl, sericite and chlorite aggregates replacing juvenile vitroclasts; Qtz, quartz; FK, K-feldspar; AL, andesitic lithoclast with seriate and porphyritic texture; RL, rhyolite lithoclasts).

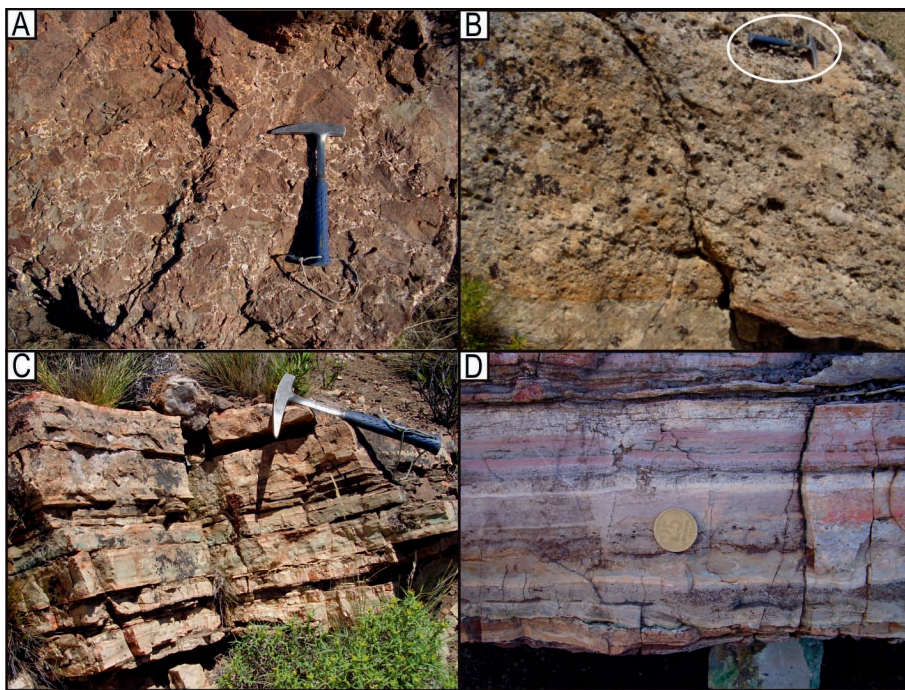


Fig. 10. Volcanic and sedimentary units of the Upper Member. (a) Stockworks and hydraulic fractures developed in andesitic lavas overlying the Middle Member. (b) Tabular body with slightly erosive base formed by large-scale cross-stratified clast-supported conglomerates related to a coarse delta front. (c) Outcrop-scale photograph of the silicified limestone and siltstone deposits that originated in a shallow lacustrine environment. (d) Detail of the lacustrine deposits.

clearly dominated by normal tectonic subsidence along with the presence of volcanic episodes coeval with the continental sedimentation (Fig. 12a). In this sense, the characteristics of the volcanic and sedimentary units that form the Lower Member are similar to those described in many stratovolcanoes (Fig. 12a; see Cas & Wright 1987; Palmer *et al.* 1993; Schneider & Fisher 1998; Belousov *et al.* 1999; Davidson & De Silva 2000; Zanchetta *et al.* 2004; Shea *et al.* 2008).

Subsidence conditions during the deposition of the Middle Member changed drastically, implying the establishment of a completely different depositional regime inside the depocentre. The first ignimbrite

(Unit A) overlies the stratovolcano sequence (i.e. the Lower Member) at a sharp depocentre-scale contact surface (Fig. 6b). This suggests the existence of a long depositional hiatus (indicating that there was no temporal relation between the stratovolcanoes and the emplacement of the Middle Member ignimbrites), and of a long period of degradation of the stratovolcanoes (Fig. 12b) before the major explosive events. Immediately after the deposition of Unit A, the emplacement of the second ignimbrite followed after a brief interruption. Thus, the depocentre was filled in a relatively short time, indicating a rapid subsidence, which may be explained as resulting from a caldera-like collapse

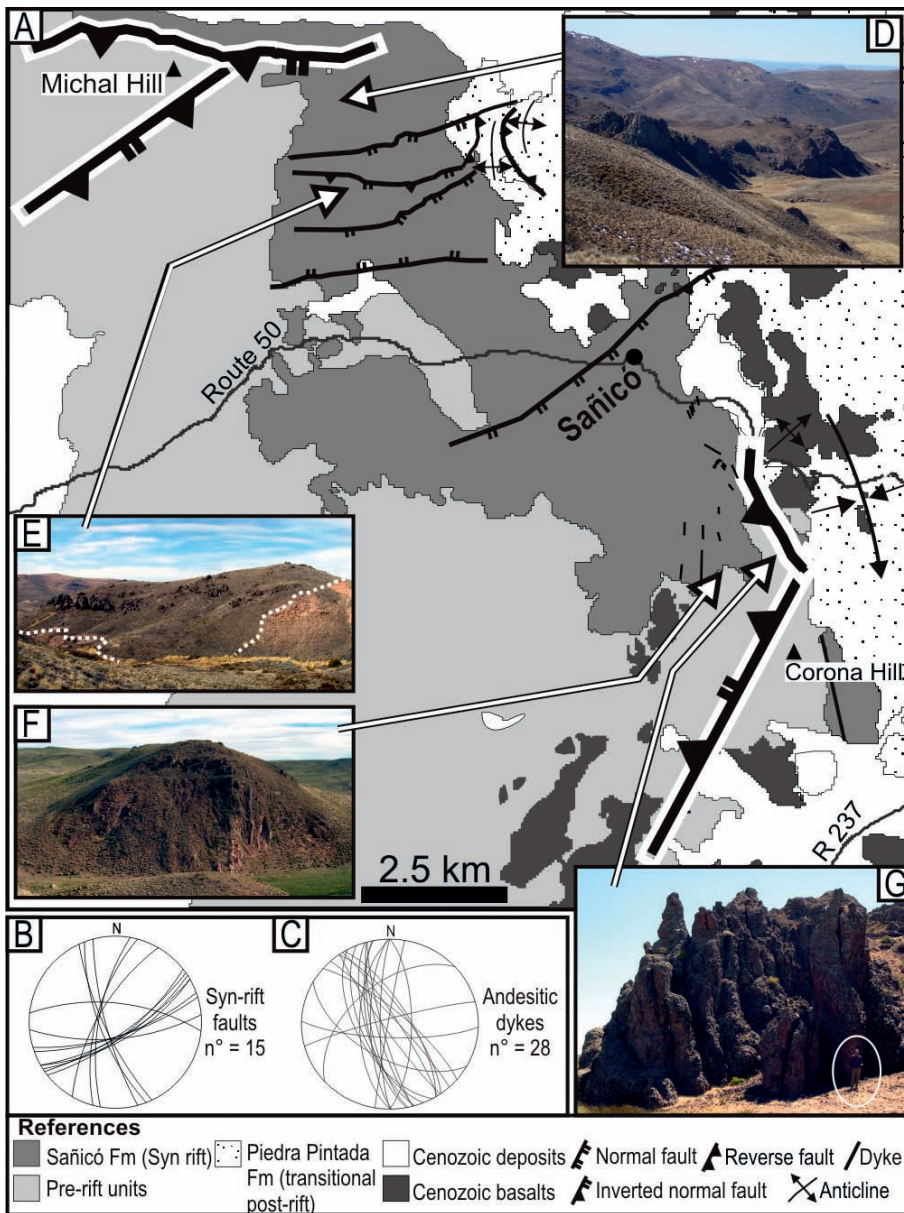


Fig. 11. Structural features of the Sañicó depocentre and their relation to the volcanic system. (a) Simplified geological map showing the main synrift tectonic structures. (b) Rose diagram of the large- and meso-scale extensional or inverted normal faults that controlled the synrift sequence. (c) Rose diagram of the longitudinal andesitic dyke swarms corresponding to extensional fractures oblique to the master faults of the sub-basin. (d, e) Rhyodacitic neck and extrusive lava dome related to ENE–WSW-trending fractures. (f, g) Rhyodacitic cryptodome and neck associated with NNW–SSE-trending faults.

that occurred along the main tectonic faults that were controlling basin subsidence. Caldera collapse probably took place in a piecemeal fashion (see Lipman 1997, 2000; Moore & Kokelaar 1997, 1998), as seems to be indicated by the spatial distribution of the ignimbrites and their thickness and facies variations, in particular the abrupt thickness variations of Unit A, which shows a highly disturbed lower contact and a relatively flat and continuous upper contact (Fig. 7a and b). This caldera event represents a minimum volume of 20 km³, as indicated by the total volume of preserved ignimbrites. However, this volume might have been much larger, even an order of magnitude higher (see Gravley *et al.* 2007), if we consider the strong effects of post-depositional erosion and tectonic processes on the original deposits, which caused the disappearance of any extra-caldera deposits and part of the intra-caldera sequence. Moreover, the vertical extent of the collapse must have been much larger than the total thickness of the preserved ignimbrites, as suggested by the characteristics of the Upper Member deposits, which are clearly compatible with deposition in a deep post-eruptive depression. The absence of proximal facies in the central zone of the

sub-basin and the occurrence of co-genetic post-caldera felsic cryptodomes and lava domes (see D'Elia *et al.* 2012a, b) related to fractures in marginal zones (Fig. 12) suggest that the ignimbritic eruptions originated from fissural vents located along the margins of the depocentre. This is also confirmed by the emplacement of lithic lag breccias, corresponding to events of opening or enlargement of vents (see Wright & Walker 1977; Druitt & Sparks 1982, 1984; Pittari *et al.* 2008), close to the marginal fault zones (Fig. 7). These characteristics, together with the absence of fallout deposits preceding the emplacement of the ignimbrites, suggest that the tectonic faults and extensional environment may have conditioned the rapid onset of caldera subsidence along with a high discharge rate, in which eruption rapidly evolved into a pyroclastic flow phase (see Charlier *et al.* 2003; Gravley *et al.* 2007; Martí *et al.* 2009; Allan *et al.* 2012).

The Upper Member unconformably overlies the caldera deposits and shows a decrease in the volume of volcanic rocks, which form less than 52% in volume. A reduction of its total thickness and lateral extent compared with previous events can also be observed, thus

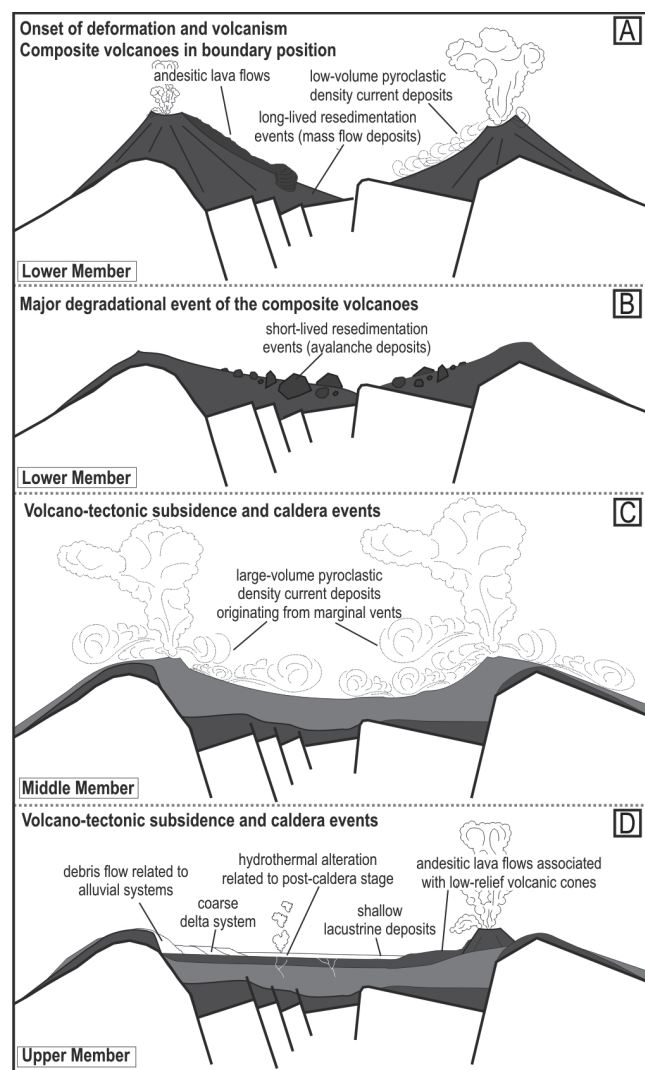


Fig. 12. Conceptual model showing the evolution of the Sañicó graben–caldera. (a) Composite volcanoes located in the boundaries of the Sañicó depocentre. (b) Major degradational events of the composite volcanoes indicating a significant hiatus before the subsequent stage. (c) Caldera event developed in the mid-synrift stage (i.e. Middle Member). (d) Low-relief volcanic cones and organized sedimentary environments (i.e. coarse delta and lacustrine environments) developed in a post-caldera stage (i.e. Upper Member).

suggesting that after the caldera event the depocentre recovered a normal tectonic subsidence. During this period, andesitic and rhyolitic lava units, together with epiclastic and carbonate sedimentary deposits, were asymmetrically distributed within the depocentre (Fig. 12d). The distribution of rhyolitic lava flows and domes associated with the bounding faults of the depocentre (Fig. 11) suggests that post-caldera vents occurred at or near the caldera margins. The sedimentary environment during this stage, characterized by alluvial, deltaic and lacustrine sedimentation, reached the highest degree of development of the whole synrift succession (D'Elia *et al.* 2012b).

Conclusions

The study of the stratigraphy and structure of the Sañicó depocentre has revealed that caldera-forming processes were superimposed on tectonic subsidence during the evolution of that portion of the

Neuquén rift basin. Following the first stage in the evolution of the extensional depocentre, in which a volcano-sedimentary succession typical of a stratovolcano apron was deposited in the depocentre, a caldera-like episode occurred, controlled by the same rift master fault and by secondary faults responsible for the tectonic structure and subsidence of the depocentre. This caldera collapse event was associated with the eruption of two large ignimbrites and it developed in a piecemeal fashion, allowing the deposition of one-third of the total thickness of the volcanic synrift succession in that portion of the basin. Subsequently, the Sañicó depocentre recovered its normal tectonic subsidence, allowing the development of well-organized fluvial and lacustrine sedimentation with some associated volcanic episodes inside the caldera depression.

These results show the complex interplay that existed between extensional tectonics and volcanism. During the evolution of the Lower and Upper members of the Sañicó Formation volcanism was abundant but was outstripped by tectonism, being subordinate to tectonic structures, whereas in the Middle Member volcano-tectonic structures combined with the emplacement of the large-volume ignimbrites totally controlled the synrift progress. Thus, tectonism and volcanism were expressed in different styles and magnitudes, with the activation of the tectonic structures as volcano-tectonic structures, and the sudden change from normal long-term rift subsidence to a high subsidence rate, coinciding with the caldera event, which caused a major shift in the depositional rift environment.

This new interpretation of the Sañicó sub-basin implies a drastic change in the current knowledge of the Neuquén basin and in its implications for hydrocarbon prospecting there. In addition, the results obtained confirm that, as far as their dynamics is concerned, tectonically controlled collapse calderas differ from those typically formed on composite volcanoes, in the sense that the massive withdrawal of the associated magma chamber and caldera subsidence are directly controlled by the same fault systems that define the basin structure, and not by a newly formed ring fault system.

The authors would like to thank the people of the Sañicó area for their support and hospitality. Our thanks go to G. Aguirre-Díaz and an anonymous reviewer for their constructive and helpful reviews. This research was funded by the Agencia Nacional de Promoción Científica y Tecnológica (PICT 07-8451–PICT 2530-BID 1728/OC-AR), the Consejo Nacional de Investigaciones Científicas y Técnicas (CONICET-Argentina), the Consejo Superior de Investigaciones Científicas (CSIC-España), and a MICINN grant CGL2010-22022-C02-02

References

- ABEBE, B., ACOCCELLA, V., KORME, T. & AYALEW, D. 2007. Quaternary faulting and volcanism in the Main Ethiopian Rift. *Journal of African Earth Sciences*, **48**, 115–124.
- ACOCCELLA, V., FUNICIELLO, R., MAROTTA, E., ORSI, G. & DE VITA, S. 2004. The role of extensional structures on experimental calderas and resurgence. *Journal of Volcanology and Geothermal Research*, **129**, 199–217.
- ACOCCELLA, V. 2007. Understanding caldera structure and development: An overview of analogue models compared to natural calderas. *Earth-Science Reviews*, **85**, 125–160.
- ACOCCELLA, V., FUNICIELLO, R., MAROTTA, E., ORSI, G. & DE VITA, S. 2004. The role of extensional structures on experimental calderas and resurgence. *Journal of Volcanology and Geothermal Research*, **129**, 199–217.
- AGUIRRE-DÍAZ, G.J., LABARTHE-HERNÁNDEZ, G., TRISTÁN-GONZÁLEZ, M., NIETO-OBREGÓN, J. & GUTIÉRREZ-PALOMARES, I. 2008. The ignimbrite flare-up and graben caldera of the Sierra Madre Occidental, Mexico. In: GOTTMANN, J. & MARTÍ, J. (eds) *Caldera Volcanism: Analysis, Modeling and Response*. Amsterdam, Elsevier, 143–174.
- ALLAN, A.S.R., WILSON, C.J.N., MILLET, M.-A. & WYSOCZANSKI, R.J. 2012. The invisible hand: tectonic triggering and modulation of a rhyolitic supereruption. *Geology*, doi:10.1130/G32969.1.
- ALLEN, S.R. 2001. Reconstruction of a major forming eruption from pyroclastic deposit characteristics: Kos Plateau Tuff, eastern Aegean Sea. *Journal of Volcanology and Geothermal Research*, **105**, 141–162.

- ALLEN, S.R. & CAS, R.A.F. 1998. Rhyolitic fallout and pyroclastic density current deposits from a phreatoplinian eruption in the eastern Aegean Sea, Greece. *Journal of Volcanology and Geothermal Research*, **86**, 219–251.
- ALLEN, S.R., STADLBAUER, E. & KELLER, J. 1999. Stratigraphy of the Kos Plateau Tuff: Product of a major Quaternary explosive rhyolitic eruption in the eastern Aegean, Greece. *International Journal of Earth Sciences*, **88**, 132–156.
- BECHIS, F., GIAMBIAGI, L., GARCÍA, G., LANÉS, S., CRISTALLINI, E. & TUNIK, M. 2010. Kinematic analysis of a transtensional fault system: the Atuel depocenter of the Neuquén basin, southern Central Andes, Argentina. *Journal of Structural Geology*, **32**, 886–899.
- BELOUSOV, A., BELOUSOVA, M. & VOIGHT, B. 1999. Multiple edifice failures, debris avalanches and associated eruptions in the Holocene history of Shiveluch volcano, Kamchatka, Russia. *Bulletin of Volcanology*, **61**, 324–342.
- BEST, M.G. & CHRISTIANSEN, E.H. 2001. *Igneous Petrology*. Blackwell Science, Malden, MA.
- BRANNEY, M.J. & KOKELAAR, B.P. 1994. Volcanotectonic faulting, soft-state deformation, and rheomorphism of tuffs during development of a piecemeal caldera, English Lake District. *Geological Society of America Bulletin*, **106**, 507–530.
- BRANNEY, M.J. & KOKELAAR, P. (eds) 2002. *Pyroclastic Density Currents and the Sedimentation of Ignimbrites*. Geological Society, London, Memoirs, **27**.
- CAS, R.A.F. & WRIGHT, J.W. 1987. *Volcanic Successions. Modern and Ancient*. Chapman & Hall, London.
- CHARLIER, B.L.A., PEATE, D.W., WILSON, C.J.N., LOWENSTERN, J.B., STOREY, M. & BROWN, J.A. 2003. Crystallisation ages in coeval silicic magma bodies: ^{238}U – ^{230}Th disequilibrium evidence from the Rotoiti and Earthquake Flat eruption deposits, Taupo Volcanic Zone, New Zealand. *Earth and Planetary Science Letters*, **206**, 441–457.
- COLE, J.W., SPINKS, K.D., DEERING, C.D., NAIRN, I.A. & LEONARD, G.S. 2010. Volcanic and structural evolution of the Okataina Volcanic Centre; dominantly silicic volcanism associated with the Taupo Rift, New Zealand. *Journal of Volcanology and Geothermal Research*, **190**, 123–135.
- COLE, R.B., MILNER, D.M. & SPINKS, K.D. 2005. Calderas and caldera structures: a review. *Earth-Science Reviews*, **69**, 1–26.
- COLGAN, J.P., JOHN, D.A. & HENRY, C.D. 2008. Large-magnitude Miocene extension of the Caetano caldera, southern Shoshone and northern Toiyabe Ranges. *Geosphere*, **4**, 107–130, doi:10.1130/GES00115.1.
- COOPER, M.A. & WILLIAMS, G.D. (eds) 1989. *Inversion Tectonics*. Geological Society, London, Special Publications, **44**.
- COSTA, F. 2008. Residence times of silicic magmas associated with calderas. In: GOTTMANN, J. & MARTÍ, J. (eds) *Caldera Volcanism: Analysis, Modeling and Response*. Amsterdam, Elsevier, 1–55.
- CRISTALLINI, E.O., BOTTESI, G., GAVARRINO, A., RODRIGUEZ, L., TOMEZZOLI, R.N. & COMERON, R. 2006. Synrift geometry of the Neuquén Basin in the north-eastern Neuquén Province, Argentina. In: KAY, S.M. & RAMOS, V.A. (eds) *Evolution of the Andean Margin: a Tectonic and Magmatic View from the Andes to the Neuquén Basin (35°–39°S lat)*. Geological Society of America, Special Papers, **407**, 147–161.
- CUMMINGS, M.J., EVANS, J.G., FERNS, M.L. & LEES, K.R. 2000. Stratigraphic and structural evolution of the middle Miocene synvolcanic Oregon–Idaho graben. *Geological Society of America Bulletin*, **112**, 668–682.
- DAMBORENEA, S.E. & MANCENIDO, M.O. 1993. Piedra Pintada. In: RICCARDI, A.C. & DAMBORENEA, S.E. (eds) *Léxico Estratigráfico de la Argentina, Volumen IX, Jurásico: 313*. Asociación Geológica Argentina, Serie B (Didáctica y Complementaria), **21**, 313–316.
- DAVIDSON, J. & DE SILVA, S. 2000. Composite volcanoes. In: SIGURDSSON, H., HOUGHTON, B., MCNUTT, S.R., RYMER, H. & STIX, J. (eds) *Encyclopedia of Volcanoes*. Academic Press, San Diego, CA, 663–682.
- D'ELIA, L., MURAVCHIK, M., FRANZESE, J.R. & BILMES, A. 2012a. Syn-rift volcanism of the Neuquén Basin, Argentina: Relationships with the Late Triassic–Early Jurassic evolution of the Andean margin. *Andean Geology*, **39**, 106–132.
- D'ELIA, L., MURAVCHIK, M., FRANZESE, J.R. & LÓPEZ, L. 2012b. Tectonostratigraphic analysis of the Late Triassic–Early Jurassic syn-rift sequence of the Neuquén Basin in the Sañicó depocentre, Neuquén Province, Argentina. *Andean Geology*, **39**, 133–157.
- DRUITT, T.H. & SPARKS, R.S.J. 1982. A proximal ignimbrite breccia facies on Santorini, Greece. *Journal of Volcanology and Geothermal Research*, **13**, 147–171.
- DRUITT, T.H. & SPARKS, R.S.J. 1984. On the formation of calderas during ignimbrite eruptions. *Nature*, **310**, 679–681.
- FOLGUERA, A. & RAMOS, V. 2011. Repeated eastward shifts of arc magmatism in the Southern Andes: a revision to the long-term pattern of Andean uplift and magmatism. *Journal of South American Earth Sciences*, **32**, 531–546.
- FRANZESE, J.R. & SPALLETTI, L.A. 2001. Late Triassic–early Jurassic continental extension in southwestern Gondwana: Tectonic segmentation and pre-break-up rifting. *Journal of South American Earth Sciences*, **14**, 257–270.
- FRANZESE, J.R., SPALLETTI, L.A., GÓMEZ PÉREZ, I. & MACDONALD, D. 2003. Tectonic and paleoenvironmental evolution of Mesozoic sedimentary basins along the Andean foothills of Argentina (32°–54°S). *Journal of South American Earth Science*, **16**, 81–90.
- FRANZESE, J.R., VEIGA, G.D., SCHWARZ, E. & GÓMEZ-PÉREZ, I. 2006. Tectonostratigraphic evolution of a Mesozoic graben border system: The Chachil depocentre, southern Neuquén Basin, Argentina. *Journal of the Geological Society, London*, **163**, 707–721.
- FRANZESE, J.R., VEIGA, G.D., MURAVCHIK, M., ANCHETA, D. & D'ELIA, L. 2007. Estratigrafía de 'sin-rift' (Triásico Superior–Jurásico Inferior) de la Cuenca Neuquina en la sierra de Chacaico, Neuquén, Argentina. *Revista Geológica de Chile*, **34**, 49–62.
- FRENGUELL, J. 1948. Estratigrafía y Edad del llamado 'Retico' en la Argentina. *Anales de la Sociedad Argentina de Estudios Geográficos, GAEA*, **8**, 159–309.
- GALLI, C.A. 1969. *Descripción Geológica de la Hoja 38c, Piedra del Águila (provincias del Neuquén y Río Negro)*. Dirección Nacional de Geología y Minería, Buenos Aires, Boletín, **111**.
- GAWTHORPE, R.L. & LEEDER, M.R. 2000. Tectono-sedimentary evolution of active extensional basins. *Basin Research*, **12**, 195–218.
- GIAMBIAGI, L.B., BECHIS, F., GARCÍA, V.H. & CLARK, A. 2008. Temporal and spatial relationships of thick- and thin-skinned deformation in the Malargüe fold and thrust belt, Southern Central Andes. *Tectonophysics*, **459**, 123–139.
- GRAVLEY, D.M., WILSON, C.J.N., LEONARD, G.S. & COLE, J.W. 2007. Double trouble: paired ignimbrite eruptions and collateral subsidence in the Taupo Volcanic Zone, New Zealand. *Geological Society of America Bulletin*, **119**, 18–30.
- GULISANO, C. & PANDO, G.A. 1981. Estratigrafía y facies de los depósitos jurásicos entre Piedra del Águila y Sañicó, Departamento Collón Curá, Provincia del Neuquén. In: NULLO, F.E., PLOSKIEWICZ, V. & MÁRIN, G. (eds) *VIII Congreso Geológico Argentino, San Luis, Actas*, **3**, 553–577.
- HOWELL, J.A. & FLINT, S.S. 1996. A model for high resolution sequence stratigraphy within extensional basins. In: HOWELL, J.A. & AITKEN, J.F. (eds) *High-Resolution Sequence Stratigraphy: Innovations and Applications*. Geological Society, London, Special Publications, **104**, 37–49.
- HOWELL, J.A., SCHWARZ, E., SPALLETTI, L.A. & VEIGA, G.D. 2005. The Neuquén Basin: An overview. In: VEIGA, G.D., SPALLETTI, L.A., HOWELL, J.A. & SCHWARZ, E. (eds) *The Neuquén Basin, Argentina: A Case Study in Sequence Stratigraphy and Basin Dynamics*. Geological Society, London, Special Publications, **252**, 1–14.
- JACKSON, C.A.L., GAWTHORPE, R.L., CARR, I.D. & SHARP, I.R. 2005. Normal faulting as a control on the stratigraphic development of shallow marine syn-rift sequences: The Nukhul and Lower Rudeis Formations, Hammam Faraun fault blocks, Suez Rift, Egypt. *Sedimentology*, **52**, 313–338.
- JANECKE, S.U., HAMMOND, B.F., SNEE, L.W. & GEISSMAN, J.W. 1997. Rapid extension in an Eocene volcanic arc: structure and paleogeography of an intra-arc half-graben in central Idaho. *Geological Society of America Bulletin*, **109**, 253–267.
- LEGARRETA, L., VILLAR, H.J., CRUZ, C.E., LAFFITTE, G.A. & VARADÉ, R. 2008. Revisión integrada de los sistemas generadores, estilos de migración–entrapamiento y volumetría de hidrocarburos en los distritos productivos de la Cuenca Neuquina. In: CRUZ, C.E., RODRÍGUEZ, J.F. & VILLAR, H.J. (eds) *Sistemas Petroleros de las Cuenas Andinas*. Instituto Argentino del Petróleo y del Gas, Buenos Aires, 79–108.
- LIPMAN, P.W. 1997. Subsidence of ash-flow calderas: Relation to caldera size and magma-chamber geometry. *Bulletin of Volcanology*, **59**, 198–218.
- LIPMAN, P.W. 2000. Calderas. In: SIGURDSSON, H., HOUGHTON, B., MCNUTT, S.R., RYMER, H. & STIX, J. (eds) *Encyclopedia of Volcanoes*. Academic Press, San Diego, CA, 643–662.
- MARTÍ, J. 1991. Caldera-like structures related to Permo-Carboniferous volcanism of the Catalan Pyrenees (NE Spain). *Journal of Volcanology and Geothermal Research*, **45**, 173–186.
- MARTÍ, J. 1996. Genesis of crystal-rich volcanoclastic facies in the Permian red beds of the Central Pyrenees (NE Spain). *Sedimentary Geology*, **106**, 1–19.
- MARTÍ, J., GEYER, A. & FOLCH, A. 2009. A genetic classification of collapse calderas based on field studies and analogue and theoretical modeling. In: THORDARSON, T., SELF, S., LARSEN, G., ROWLAND, S.K. & HOSKULDSSON, A. (eds) *Studies in Volcanology: The Legacy of George Walker*. Geological Society, London, Special Publications of IAVCEI, **2**, 249–266.
- MCCLAY, K. 1995. The geometries and kinematics of inverted fault systems: a review of analogue model studies. In: BUCHANAN, J.G. & BUCHANAN, P.G. (eds) *Basin Inversion*. Geological Society, London, Special Publications, **88**, 97–118.
- MOORE, I. & KOKELAAR, P. 1997. Tectonic influences in piecemeal caldera collapse at Glencoe Volcano, Scotland. *Journal of the Geological Society, London*, **154**, 765–768.
- MOORE, I. & KOKELAAR, P. 1998. Tectonically controlled piecemeal caldera collapse: a case study of Glencoe volcano, Scotland. *Geological Society of America Bulletin*, **110**, 1448–1466.
- MORA-KLEPEIS, G. & McDOWELL, F.W. 2004. Late Miocene calc-alkalic volcanism in northwestern Mexico: an expression of rift or subduction-related magmatism? *Journal of South American Earth Science*, **17**, 297–310.

- MOREL, E.M. & GANUZA, D.G. 2002. Paso Flores. In: STIPANICIC, P.N. & MARSISCANO, C.A. (eds) *Léxico Estratigráfico de la Argentina, Volumen VIII, Triásico: 208*. Asociación Geológica Argentina, Serie B (Didáctica y Complementaria), **26**, 208–209.
- MORLEY, C.K. 1999. Basin evolution trends in East Africa. In: MORLEY, C.K. (ed.) *Geoscience of Rift Systems—Evolution of East Africa*. American Association of Petroleum Geologists, Studies in Geology, **44**, 131–150.
- MORLEY, C.K., HARANYA, C., PHOOSONGSEE, W., PONGWAPEE, S., KORNSAWAN, A. & WONGANAN, N. 2004. Activation of rift oblique and rift parallel preexisting fabrics during extension and their effect on deformation style: Examples from the rifts of Thailand. *Journal of Structural Geology*, **26**, 1803–1829.
- MOUSTAFA, A.R. 2002. Controls on the geometry of transfer zones in the Suez rift and northwest Red Sea. Implications for the structural geometry of rift systems. *AAPG Bulletin*, **86**, 979–1002.
- MURAVCHIK, M., D'ELIA, L., BILMES, A. & FRANZESE, J.R. 2008. Caracterización de los depocentros de rift (Ciclo Precuyano) aflorantes en el sector sudoccidental de la Cuenca Neuquina, Argentina. In: SCHIUMA, M. (ed.) *VII Congreso de Exploración y Desarrollo de Hidrocarburos, Trabajos Técnicos*. Instituto Argentino del Petróleo y del gas, Buenos Aires, 457–470.
- MURAVCHIK, M., D'ELIA, L., BILMES, A. & FRANZESE, J.R. 2011. Syn-eruptive/inter-eruptive relations in the syn-rift deposits of the Precuyano Cycle, Sierra de Chacaico, Neuquén Basin, Argentina. *Sedimentary Geology*, **238**, 132–144.
- NEGRETE-ARANDA, R. & CANÓN-TAPIA, E. 2008. Post subduction volcanism in the Baja California Peninsula, Mexico: The effects of tectonic reconfiguration in volcanic systems. *Lithos*, **102**, 392–414.
- NÉMETH, K. & ULRIKE, M. 2007. *Practical Volcanology. Lecture notes for understanding volcanic rocks from field-based studies*. Geological Institute of Hungary, Occasional Papers, **27**.
- PALMER, B.A., PURVES, A.M. & DONOHUE, S.L. 1993. Controls on accumulation of a volcanoclastic fan, Ruapehu composite volcano, New Zealand. *Bulletin of Volcanology*, **55**, 176–189.
- PÁNGARO, F., CORBERA, R., CARBONE, O. & HINTERWIMMER, G. 2002. Los reservorios del Precuyano. In: SCHIUMA, M., HINTERWIMMER, G. & VERGANI, G.D. (eds) *Rocas Reservorio de las Cuencas Productivas Argentinas*. Instituto Argentino del Petróleo y del Gas, Buenos Aires, 229–254.
- PÁNGARO, F., PEREIRA, D.M. & MICUCCI, E. 2009. El sinrift de la dorsal de Huincul, Cuenca Neuquina: evolución y control sobre la estratigrafía y estructura del área. *Revista de la Asociación Geológica Argentina*, **65**, 265–277.
- PETRINOVIC, I.A., MARTÍ, J., AGUIRRE-DÍAZ, G.J., GUZMÁN, S., GEYER, A. & SALADO PAZ, N. 2010. The Cerro Aguas Calientes caldera, NW Argentina: an example of a tectonically controlled, polygenetic collapse caldera, and its regional significance. *Journal of Volcanology and Geothermal Research*, **194**, 15–26.
- PITTARI, A., CAS, R.A.F., WOLFF, J.A., NICHOLS, H.J. & MARTÍ, J. 2008. The use of lithic clast distributions in pyroclastic deposits to understand pre- and syn-caldera collapse processes: a case study of the Abrigo Ignimbrite, Tenerife, Canary Islands. In: GOTTMANN, J. & MARTÍ, J. (eds) *Caldera Volcanism: Analysis, Modeling and Response*. Elsevier, Amsterdam, 97–142.
- PUSKAS, C.M., SMITH, R.B., MEERTENS, C.M. & CHANG, W.L. 2007. Crustal deformation of the Yellowstone–Snake River Plain volcano-tectonic system: Campaign and continuous GPS observations, 1987–2004. *Journal of Geophysical Research*, **112**, B03401.
- RAMOS, V.A. 2009. Anatomy and global context of the Andes: main geologic features and the Andean orogenic cycle. In: KAY, S.M., RAMOS, V.A. & DICKINSON, W.R. (eds) *Backbone of the Americas: Shallow Subduction, Plateau Uplift, and Ridge and Terrane Collision*. Geological Society of America, Memoirs, **204**, 31–65, doi:10.1130/2009.1204(02).
- ROWLAND, J.V. & SIBSON, R.H. 2001. Extensional fault kinematics within the Taupo Volcanic Zone, New Zealand: Soft-linked segmentation of a continental rift system. *Journal of Geophysical Research*, **44**, 271–283.
- ROWLAND, J.V., WILSON, C.J.N. & GRAVLEY, D.M. 2010. Spatial and temporal variations in magma-assisted rifting, Taupo Volcanic Zone, New Zealand. *Journal of Volcanology and Geothermal Research*, **190**, 89–108.
- SCHIUMA, M. & LLAMBIAS, E.J. 2008. New ages and chemical analysis on Lower Jurassic volcanism close to the Huincul High, Neuquén. *Revista de la Asociación Geológica Argentina*, **63**, 644–652.
- SCHLISCHE, R.W. 1991. Half-graben basin filling models: new constraints on continental extensional basin development. *Basin Research*, **3**, 123–141.
- SCHLISCHE, R.W. 1992. Structural and stratigraphic development of the Newark extensional basin, eastern North America: Evidence for the growth of the basin and its bounding structures. *Geological Society of America Bulletin*, **104**, 1246–1263.
- SCHLISCHE, R.W. & ANDERS, M.H. 1996. Stratigraphic effects and tectonic implications of the growth of normal faults and extensional basins. In: DUBIEL, R.F., POTTER, C.J., GOOD, S.C. & SNEE, L.W. (eds) *Reconstructing the History of Basin and Range Extension Using Sedimentology and Stratigraphy*. Geological Society of America, Special Papers, **303**, 183–203.
- SCHNEIDER, J. & FISHER, R.V. 1998. Transport and emplacement mechanisms of large volcanic debris avalanches: Evidence from the northwest sector of Cantal Volcano (France). *Journal of Volcanology and Geothermal Research*, **83**, 141–165.
- SESANA, F.L. 1968. Rasgos petrológicos de la comarca de Río Chico, Río Negro. *Terceras Jornadas Geológicas Argentinas, Actas*, **3**, 99–105.
- SHEA, T., VAN WYK, DE, VRIES, B. & PILATO, M. 2008. Emplacement mechanisms of contrasting debris avalanches at Volcán Mombacho (Nicaragua), provided by structural and facies analysis. *Bulletin of Volcanology*, **70**, 899–921.
- SMITH, G.A. 1986. Coarse-grained nonmarine volcanoclastic sediment—terminology and depositional process. *Geological Society of America Bulletin*, **97**, 1–10.
- SMITH, G.A. 1987. The influence of explosive volcanism on fluvial sedimentation: the Deschutes Formation (Neogene) in Central Oregon. *Journal of Sedimentary Petrology*, **57**, 613–629.
- SMITH, G.A. & LOWE, D.R. 1991. Lahars: volcano-hydrologic events and deposition in the debris flow-hyperconcentrated flow continuum. In: FISHER, R.V. & SMITH, G.A. (eds) *Sedimentation in Volcanic Settings*. Society of Economic Paleontologists and Mineralogists, Special Publications, **45**, 59–70.
- SPALLETTI, L.A., FRANZESE, J.R., MOREL, E., D'ELIA, L., ZÚÑIGA, A. & FANNING, C.M. 2010. Consideraciones acerca de la sedimentología, paleobotánica y geocronología de la Formación Piedra del Águila (Jurásico Inferior, Neuquén, República Argentina). *Revista de la Asociación Geológica Argentina*, **66**, 305–313.
- SPINKS, K.D., ACOCELLA, V., COLE, J.W. & BASSETT, K.N. 2005. Structural control of volcanism and caldera development in the transtensional Taupo Volcanic Zone, New Zealand. *Journal of Volcanology and Geothermal Research*, **144**, 7–22.
- STIPANICIC, P.N. 1967. Consideraciones sobre las edades de algunas fases magmáticas del Neopaleozoico y Mesozoico. *Revista de la Asociación Geológica Argentina*, **22**, 101–133.
- STIPANICIC, P.N. 1969. El avance de los conocimientos del Jurásico argentino a partir del esquema de Groeber. *Revista de la Asociación Geológica Argentina*, **24**, 367–388.
- STIPANICIC, P.N., RODRIGO, F., BAULIES, O.L. & MARTÍNEZ, C.G. 1968. Las formaciones presenonianas en el denominado Macizo Nordpatagónico y regiones adyacentes. *Revista de la Asociación Geológica Argentina*, **23**, 67–98.
- SULPIZIO, R. & DELLINO, P. 2008. Sedimentology, depositional mechanisms and pulsating behaviour of pyroclastic density currents. In: GOTTMANN, J. & MARTÍ, J. (eds) *Caldera Volcanism: Analysis, Modeling and Response*. Elsevier, Amsterdam, 57–96.
- SULPIZIO, R., MELE, D., DELLINO, P. & LA VOLPE, L. 2007. High variability of sedimentology and physical properties of pyroclastic density currents during complex Subplinian eruptions: The example of the AD 472 (Pollena) eruption of Somma–Vesuvius, Italy. *Sedimentology*, **54**, 607–635.
- VARELA, R., DALLA SALDA, L., CINGOLANI, C. & GÓMEZ, V. 1991. Estructura, petrología y geocronología del basamento de la región del Río Limay del Río Negro y Neuquén, Argentina. *Revista Geológica de Chile*, **18**, 147–163.
- VARELA, R., BASEI, M.A.S., CINGOLANI, C.A., SIGA, O., JR. & PASSARELLI, C.R. 2005. El basamento cristalino de los Andes norpatagónicos en Argentina: geocronología e interpretación tectónica. *Revista Geológica de Chile*, **32**, 167–187.
- VERGANI, G.D., TANKARD, A.J., BELOTTI, H.J. & WEISINK, H.J. 1995. Tectonic evolution and paleogeography of the Neuquén basin, Argentina. In: TANKARD, A.J., SUÁREZ, S.R. & WELSINK, H.J. (eds) *Petroleum Basins of South America*. American Association of Petroleum Geologists, Memoirs, **62**, 383–402.
- VOLKHEIMER, W. 1964. Estratigrafía de la zona extraandina del departamento de Cushamen (Chubut) entre los paralelos 42° y 42°30' y los meridianos 70° y 71°. *Revista de la Asociación Geológica Argentina*, **19**, 85–107.
- WILSON, C.J.N., HOUGHTON, B.F., MCWILLIAMS, M.O., LANPHERE, M.A. & WEAVER BRIGGS, R.M. S.D. 1995. Volcanic and structural evolution of Taupo Volcanic Zone, New Zealand: A review. *Journal of Volcanology and Geothermal Research*, **68**, 1–28.
- WRIGHT, J.V. & WALKER, G.P.L. 1977. The ignimbrite source problem: Significance of a co-ignimbrite lag-fall deposit. *Geology*, **5**, 729–732.
- ZANCHETTA, G., SULPIZIO, R. & DI VITO, M.A. 2004. The role of volcanic activity and climate in alluvial fan growth at volcanic areas: An example from southern Campania (Italy). *Sedimentary Geology*, **168**, 249–280.
- ZIEGLER, P.A. & CLOETINGH, S. 2004. Dynamic processes controlling evolution of rifted basins. *Earth-Science Reviews*, **64**, 1–50.

Received 9 October 2012; revised typescript accepted 28 January 2013.

Scientific editing by David Pyle.